Suppression of WDM four-wave mixing crosstalk in fibre optic parametric amplifier using Raman-assisted pumping

A. Redyuk,[1,2,*] M.F.C. Stephens,[3] and N.J. Doran[3]

[1]*Institute of Computational Technologies, Novosibirsk, 6 Acad. Lavrentiev avenue, 630090, Russia*
[2]*Novosibirsk State University, Novosibirsk, 2 Pirogova street, 630090, Russia*
[3]*Aston Institute of Photonic Technologies, Aston University, Aston Triangle, Birmingham B4 7ET, UK*
[*]*redyuk@ict.sbras.ru*

Abstract: We perform an extensive numerical analysis of Raman-Assisted Fibre Optical Parametric Amplifiers (RA-FOPA) in the context of WDM QPSK signal amplification. A detailed comparison of the conventional FOPA and RA-FOPA is reported and the important advantages offered by the Raman pumping are clarified. We assess the impact of pump power ratios, channel count, and highly nonlinear fibre (HNLF) length on crosstalk levels at different amplifier gains. We show that for a fixed 200 m HNLF length, maximum crosstalk can be reduced by up to 7 dB when amplifying 10x58Gb/s QPSK signals at 20 dB net-gain using a Raman pump of 37 dBm and parametric pump of 28.5 dBm in comparison to a standard single-pump FOPA using 33.4 dBm pump power. It is shown that a significant reduction in four-wave mixing crosstalk is also obtained by reducing the highly nonlinear fibre interaction length. The trend is shown to be generally valid for different net-gain conditions and channel grid size. Crosstalk levels are additionally shown to strongly depend on the Raman/parametric pump power ratio, with a reduction in crosstalk seen for increased Raman pump power contribution.

OCIS codes: (060.2320) Fiber optics amplifiers and oscillators; (190.4970) Parametric oscillators and amplifiers; (190.4380) Nonlinear optics, four-wave mixing.

References and links

1. D. J. Richardson, "Filling the light pipe," Science **330**(6002), 327–328 (2010).
2. R.-J. Essiambre, G. Kramer, P. J. Winzer, G. J. Foschini, and B. Goebel, "Capacity limits of optical fiber networks," J. Lightwave Technol. **28**(4), 662–701 (2010).
3. M. F. C. Stephens, I. D. Phillips, P. Rosa, P. Harper, and N. J. Doran, "Improved WDM performance of a fibre optical parametric amplifier using Raman-assisted pumping," Opt. Express **23**(2), 902–911 (2015).
4. X. Guo, X. Fu, and C. Shu, "Gain-saturated spectral characteristic in a Raman-assisted fiber optical parametric amplifier," Opt. Lett. **39**(12), 3658–3661 (2014).
5. C. Headley and G. P. Agrawal, *Raman Amplification in Fiber Optical Communication Systems* (Academic, 2005).
6. M. E. Marhic, *Fiber Optical Parametric Amplifiers, Oscillators and Related Devices* (Cambridge University, 2008).
7. T. Torounidis, P. A. Andrekson, and B. E. Olsson, "Fibre-optical parametric amplifier with 70-dB gain," IEEE Photon. Technol. Lett. **18**(10), 1194–1196 (2006).
8. M. E. Marhic, K. Y. K. Wong, and L. G. Kazovsky, "Wideband tuning of the gain spectra of one-pump fiber optical parametric amplifiers," IEEE J. Sel. Top. Quantum Electron. 10(5), 1133–1141 (2004).
9. J. M. C. Boggio, A. Guimarães, F. A. Callegari, J. D. Marconi, and H. L. Fragnito "Q penalties due to pump phase modulation and pump RIN in fiber optic parametric amplifiers with non-uniform dispersion," Opt. Commun. **249**(4), 451–472 (2005).
10. A. Szabo, B. J. Puttnam, D. Mazroa, A. Albuquerque, S. Shinada, and N. Wada, "Numerical comparison of WDM interchannel crosstalk in FOPA and PPLN-based PSAs," IEEE Photon. Technol. Lett. **26**(15), 1503–1506 (2014).

11. X. Guo, X. Fu, and C. Shu, "Gain saturation in a Raman-assisted fiber optical parametric amplifier," Opt. Lett. **38**(21), 4405–4408 (2013).
12. X. Guo, C. Shu, "Cross-gain modulation suppression in a Raman-assisted fiber optical parametric Amplifier," IEEE Photon. Technol. Lett. **26**(13), 1360–1363 (2014).
13. M.-C. Ho, K. Uesaka, M. Marhic, Y. Akasaka, and L. G. Kazovsky, "200-nm-Bandwidth fiber optical amplifier combining parametric and Raman gain," J. Lightwave Technol. **19**(7), 977–981 (2001).
14. S. Peiris, N. Madamopoulos, N. Antoniades, M. A. Ummy, M. Ali, and R. Dorsinville, "Optimization of gain bandwidth and gain ripple of a hybrid Raman/parametric amplifier for access network applications," Appl. Optics **51**(32), 7834–7841 (2012).
15. S. H. Wang, L. Xu, P. K. A. Wai, and H. Y. Tam, "Optimization of Raman-assisted fiber optical parametric amplifier gain," J. Lightwave Technol. **29**(8), 1172–1181 (2011).
16. N. Antoniades, G. Ellinas, I. Roudas, *WDM Systems and Networks. Modelling, Simulation, Design and Engineering* (Springer, 2012).
17. M. A. Ummy, M. F. Arend, L. Leng, N. Madamopoulos, and Roger Dorsinville, "Extending the gain bandwidth of combined Raman-parametric fiber amplifiers using highly nonlinear fiber," J. Lightwave Technol. **27**(5), 583–589 (2009).
18. G. P. Agrawal, *Nonlinear Fiber Optics* (Academic, 2001).
19. M. Morshed, L. B. Du, and A. J. Lowery, "Mid-span spectral inversion for coherent optical OFDM systems: fundamental limits to performance," J. Lightwave Technol. 31(1), 58–66 (2013).
20. A. J. Lowery, S. Wang, and M. Premaratne, "Calculation of power limit due to fiber nonlinearity in optical OFDM systems," Opt. Express **15**(20), 13282–13287 (2007).

1. Introduction

The need for higher capacity optical communications systems appears evident as worldwide demand for data continues to surge with ever more data-hungry multimedia applications and E-services appearing [1]. A logical way to increase the optical system capacity is via the development of new optical amplifiers which can provide gain at wavelengths beyond the current C/L bands catered for by the Erbium Doped Fibre Amplifier (EDFA) [2]. The Raman-Assisted Fibre Optic Parametric Amplifier (RA-FOPA) has recently been shown as a promising approach towards achieving this [3,4]. The RA-FOPA combines useful properties of discrete Raman amplifiers (low crosstalk, gain bandwidth tuneability) with those of conventional FOPAs (high gain coefficient, gain bandwidth tuneability) to offer a tuneable gain region and potentially high discrete gain. However, the impact of four-wave mixing (FWM) crosstalk on the performance of the RA-FOPA has not been characterised extensively. Here we show that the RA-FOPA offers significantly reduced FWM crosstalk compared with the conventional FOPA over all conditions whilst providing gain levels which would not be easily achievable using purely discrete Raman gain without encountering extreme problems of signal corruption and noise from double Rayleigh backscattering [5].

The conventional FOPA has been actively investigated in recent years and operates via a phase-matched degenerate four-wave mixing process between (typically) a single high power forward-travelling pump and signal(s) in highly nonlinear fibre (HNLF) [6]. Peak gain as high as 70 dB has been demonstrated [7] and a gain bandwidth of 200 nm shown [8] after optimization of HNLF and pump parameters. However, FOPA performance has also been shown to strongly depend on the quality of parametric pump [9] and to also suffer from the generation of unwanted FWM crosstalk components when amplifying WDM signals [10]. This remains a major limitation to the prospect of using FOPAs in telecoms applications. In order to improve this aspect of FOPA performance, the hybrid RA-FOPA has been proposed, based on simultaneous Raman and parametric gain within a single length of HNLF. The RA-FOPA consists of a parametric pump, co-propagated with signal(s), and a typically (although not exclusively required) backwards-travelling Raman pump. The Raman pump provides direct signal amplification through Raman scattering and indirect signal gain through amplification of the parametric pump. This approach can potentially widen the amplification bandwidth, increase overall gain and improve performance in comparison with the conventional FOPA.

The RA-FOPA has been studied theoretically, experimentally and numerically in recent years. In paper [11] gain saturation characteristics in RA-FOPA have been investigated. Different saturation characteristics have been experimentally observed and analysed using a

single continuous wave as a signal probe to measure the gain. In [12] reduction of cross-gain modulation in a RA-FOPA has been demonstrated using two 10 Gb/s RZ-OOK signals. By optimising the HNLF properties together with the pump powers and frequency tuning, gain in excess of 10 dB over a 208-nm bandwidth in fiber optical amplifier combining parametric and Raman gain has been demonstrated [13]. In paper [14], the authors have described a mathematical model and presented simulation results for the optimization of a RA-FOPA, exhibiting a bandwidth of 170 nm and low ripples. The relationship between the overall gain and different combinations of Raman and parametric pump powers have been investigated both theoretically and experimentally using a single channel signal [15].

In this paper, we extend our previous work [3] by numerically characterising a RA-FOPA using the key WDM metrics of signal gain and FWM crosstalk power at both maximum and minimum wavelengths of the amplified spectrum (encompassing both max and min crosstalk products). We vary the RA-FOPA net-gain level, Raman/parametric pump powers, pump ratios, number of WDM channels and length of HNLF in order to observe the impact on the crosstalk magnitude. We demonstrate that the RA-FOPA crosstalk is minimised by employing a combination of short HNLF length with high Raman pump power. The required net-gain is then subsequently achieved via adjustment of the parametric pump power. In practise, the Raman pump power would most likely just be increased to a suitable level before double Rayleigh effects start to dominate for that fibre.

2. Mathematical model and methodology

The RA-FOPA was simulated using the arrangement shown schematically in Fig. 1. For verification and comparison with our previous work [3], the input signals consisted of ten 100 GHz-spaced NRZ-QPSK modulated channels ranging from 193.5 to 194.4 THz and multiplexed together using a 70 GHz-wide arrayed waveguide grating (WDM1). To examine the impact of channel spacing, subsequent simulations used a doubled channel count of twenty 50 GHz-spaced signals whilst occupying the same overall bandwidth.

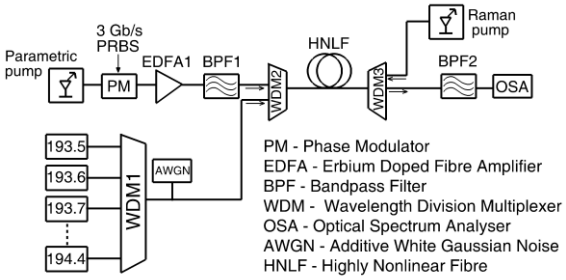

Fig. 1. Scheme of simulation for Raman-Assisted FOPA.

The QPSK modulation data was derived from two decorrelated 2^{12} pseudo-random binary bit sequences at a symbol rate of 29 Gbaud/s. A 100 kHz linewidth parametric pump laser was phase modulated using a 3 Gb/s electrical PRBS pattern to provide mitigation against stimulated Brillouin scattering (SBS) and optically amplified. The SBS process itself was not numerically simulated in this work. The power and wavelength of the pump were variable parameters used to achieve the required net-gain for all signals in either a) a conventional FOPA (C-FOPA) arrangement (no Raman) or b) a RA-FOPA arrangement. The amplified pump was bandpass filtered (BPF1) to remove amplified spontaneous emission before combination with the signals using WDM2. The combined pump/signals were transmitted through highly nonlinear fibre (HNLF) of length 0.2 km or 1 km to assess length dependence. Per-signal input power to the HNLF was fixed at a relatively high level of -10 dBm in order to generate significant FWM crosstalk under conventional FOPA operation. For RA-FOPA operation, the HNLF was additionally backward-pumped using a continuous-wave (CW)

Raman pump at 1455 nm with its power P_R an additional variable. All pumps and signals were simulated as single polarisation and perfectly aligned.

The mathematical modelling of the RA-FOPA consisted of two stages: bidirectional power analysis and field analysis [16]. In the first stage, the interaction between the signals, co-propagating parametric pump and counter propagating Raman pump was determined using the coupled balanced Eq. (1)

$$\begin{aligned} \partial P_S/\partial z &= -\alpha_S P_S + g_S P_R P_S \\ -\partial P_R/\partial z &= -\alpha_R P_R - g_R P_S P_R , \end{aligned} \qquad (1)$$

where P_R is the time-averaged power of the Raman pump, P_S is the total average power of the WDM-signals and parametric pump. g_S and g_R are the Raman coefficients, α_S and α_R are the attenuation coefficients of the parametric pump and Raman pump, respectively. We assume here that the Raman gain is constant for parametric pump and WDM-signals. This is an acceptable approximation because the bandwidth of the pump, WDM-signals and idlers is much less than the Raman gain bandwidth. The approximate solution of Eq. (1) was obtained by an iteration process using the fourth-order Runge-Kutta method [17].

In the second stage, the signal field analysis was performed by substituting the resultant power distributions along the fiber length into the nonlinear Schrödinger equation (NLSE):

$$\frac{\partial A_S}{\partial z} = \sum_{k=2}^{4} i^{k+1} \frac{\beta_k}{k!} \frac{\partial^k A_S}{\partial t^k} - \frac{\alpha_S}{2} A_S + i\gamma_S \left(|A_S|^2 + (2 - f_R) P_R \right) A_S + \frac{g_S}{2} P_R A_S , \qquad (2)$$

where A_S is the sum of complex field envelopes, f_R is the fractional contribution of the delayed Raman response, and β_k and γ_S are dispersion and Kerr coefficients, respectively. The power distributions P_R obtained from Eq. (1) were substituted along the fibre length into the Eq. (2) to take into account Raman gain. The NLSE was solved using the split-step Fourier method [18]. The HNLF parameters were as follows [3]: fiber loss was 0.8 dB/km, zero dispersion wavelength was 1564.3 nm, dispersion slope 0.084 ps·nm^{-2}·km^{-1} and nonlinear coefficient 8.2 (W·km)$^{-1}$. Values of others coefficient were as follows: $\alpha_S = \alpha_R =$ 0.8 dB/km, $g_S = 3.7$ (W·km)$^{-1}$, $g_R = 4$ (W·km)$^{-1}$, $f_R = 0.18$.

Experimental data taken from [3], and simulated output spectra of the C-FOPA and RA-FOPA are shown in Fig. 2 for the representative conditions of 20 dB net-gain and -12 dBm input power per signal. The signal at 194.4THz was removed to illustrate the crosstalk level present at this frequency. It can be seen that there is close agreement of signal power, spectral flatness and crosstalk distribution for both schemes, providing confidence in the simulation predictions.

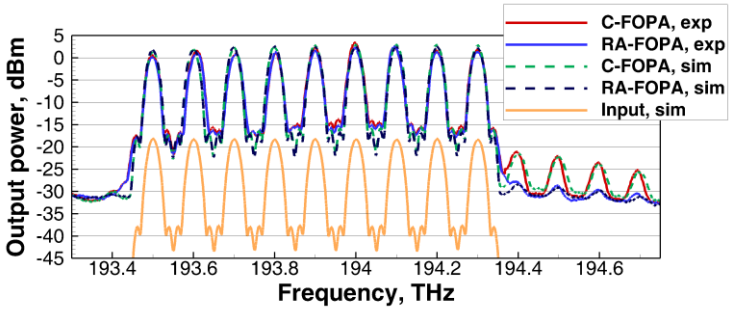

Fig. 2. Output spectra of the RA-FOPA and C-FOPA averaged over 10 runs and plotted with 12.5 GHz resolution bandwidth for -12 dBm per-signal input power and 20 dB average net-gain.

3. WDM RA-FOPA signal evolution characteristics

By employing both parametric and Raman gain in the same HNLF, the RA-FOPA offers useful advantages over an equivalent hybrid FOPA/Raman amplifier employing the same individual pump powers in separate isolated fibres of the same total length. This is because the peak of the Raman gain in the RA-FOPA can be tuned to coincide and thus provide gain to both the WDM signals and the parametric pump (PP). The latter is important because it provides additional indirect Raman amplification due to the parametric process. To understand and illustrate this phenomenon, three 20 dB net-gain scenarios were compared for the same 1 km HNLF: a) C-FOPA with 29.5 dBm PP b) RA-FOPA1 with 27.5 dBm PP & 28 dBm RP and c) RA-FOPA2 with 24.4 dBm PP & 32 dBm RP. Fig. 3 shows the evolution of the 194.4 THz signal and PP power along the length of HNLF whilst all ten WDM signals are amplified. The important difference in signal profile between the C-FOPA and RA-FOPA can clearly be seen and shows similar characteristics to single channel amplification [4].

In the RA-FOPA case, the rate of change of signal gain increases along the length of HNLF – however, in the equivalent C-FOPA the rate of change of signal gain can be seen to drop. The RA-FOPA behaviour is a direct result of the counter-propagated RP and consequential monotonic amplification of the PP. This leads to greater signal gain occurring at the output end of the fibre, suppressing unwanted nonlinear interactions between the waves involved in the parametric process along the fibre. It should be noted that the C-FOPA signal gain saturates under these conditions (and in reality a shorter length of HNLF would be used), but substantial margin remains for the RA-FOPA because of the parametric pump power growth along the HNLF due to the Raman amplification. In other words, Raman pumping can prevent parametric pump depletion, providing higher small signal gain compared to the C-FOPA.

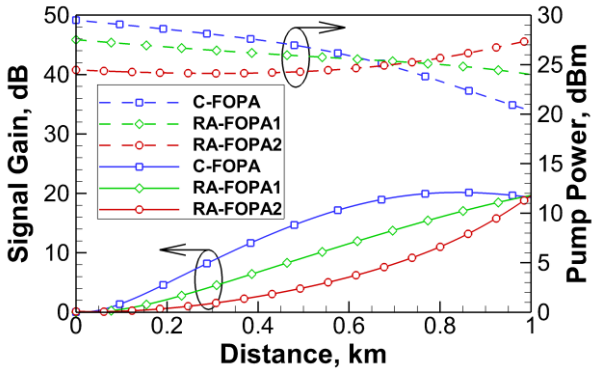

Fig. 3. Signal gain and parametric pump power along the HNLF for a C-FOPA (PP=29.5 dBm), RA-FOPA1 (PP=27.5 dBm, RP=28 dBm) and RA-FOPA2 (PP=24.4 dBm, RP=32 dBm). Per-signal input power is -10 dBm and average net-gain is 20 dB.

Assuming uniform spacing between the channels in the WDM multiplex, there are a number of FWM products generated from various combination of channels interacting along the HNLF at any particular channel frequency. The total power of the FWM waves generated at frequency f_m can be presented as

$$P_{\Sigma}^{FWM}(f_m) = \sum_{f_k} \sum_{f_j} \sum_{f_i} P_{ijk}^{FWM}(f_m), \qquad (3)$$

where frequencies involved in the FWM processes, satisfy the condition $f_m = f_i + f_j - f_k$. The strength of each component is weighted according to the mixing efficiency. Neglecting phase mismatch due to the low dispersion of the HNLF we assume equal contribution of each component to the total power. There is no loss of generality for us in supposing that the HNLF

is a lossless medium. In this case, the propagation of the signal-signal FWM waves are governed by a simple equation, derived by Morshed et al [19]

$$\frac{d\left|A_{ijk}^{FWM}(z)\right|}{dz}=\frac{D}{3}\gamma\left(P_i(z)P_j(z)P_k(z)\right)^{1/2}, \qquad (4)$$

where A_{ijk}^{FWM} is the magnitude of the FWM product, P_i, P_j and P_k are the powers of the signals at appropriate frequencies, γ is the nonlinear coefficient and D is the degeneracy factor which equals 6 for nondegenerate products and 3 for degenerate products. Finally, assuming that WDM signals have the same power profile $P^{WDM}(z)$ along HNLF, the output power of single signal-signal FWM component can be found by integrating (4) over the HNLF length and squaring, which gives:

$$P_{ijk}^{FWM}(L)=\frac{D^2}{9}\gamma^2\left(\int_0^L\left[P^{WDM}(z)\right]^{3/2}dz\right)^2. \qquad (5)$$

Equation (5) clarifies that the output power of single FWM component depends on both HNLF length and signal power profile along the fibre. Hence, there are two key parameters which have significant impact on the FOPA crosstalk performance. By decreasing the HNLF length and maintaining low signal power along the HNLF as far as possible before the required gain is achieved, the FWM crosstalk level can be significantly reduced.

Table 1 shows simulated and theoretical (based on Eq. (5) and included only signal-signal FWM components) estimation of FWM crosstalk reduction for different configuration of the RA-FOPA in comparison with the conventional C-FOPA. The integral in Eq. (5) was solved numerically using signal power profiles obtained from simulations. The net-gain here is 20 dB, HNLF length is 0.2 km and the frequency of the channel under consideration is 194.4 THz. It can be seen that there is good agreement between the two obtained estimations for this set of parameters. However, the analytical expression is based on a large number of assumptions and for simplicity we neglect the pump-signal FWM products which can make a considerable contribution to the overall crosstalk. Hence, an estimation based on Eq. (5) should always be compared with simulation results.

Table 1. Crosstalk reduction for different configuration of RA-FOPA

Parametric pump power, dBm	Raman pump power, dBm	Theoretical crosstalk reduction, dB	Simulated crosstalk reduction, dB
33.4	---	0	0
32.9	28	1.85	0.92
32.1	32	3.29	2.86
31.2	34	4.08	4.37
29.7	36	5.53	5.82
28.5	37	5.83	6.92

4. Crosstalk vs distance in RA-FOPA

A key conclusion of Section 3 is that under a fixed gain condition, the RA-FOPA can be operated with lower average (vs length) parametric pump power than the equivalent C-FOPA, and this has been experimentally shown to result in reduced FWM crosstalk [3]. To characterize the behaviour, the signal-to-crosstalk (S-to-X) power ratio was measured at different signal wavelengths across the band. This was calculated by running two simulations per measurement, both with and without the channel under test being present. When not present, the input power of the remaining nine channels was increased proportionally (0.45dB) to keep the total signal power into the HNLF constant. By doing this, the small crosstalk-reduction obtained due to removing the signal under test could be partially recovered (although not fully recovered due to the different frequency distribution between the nine and ten-signal cases).The signal power and an estimated FWM crosstalk power at the

exact signal frequency under test could then be measured and a signal-to-crosstalk ratio calculated with consistency over all simulated conditions.

Figure 4 shows the dynamics of the signal gain and signal-to-crosstalk ratio at 194.4 THz along the HNLF for 20 dB net-gain and for two different lengths of HNLF. The signal at 194.4 THz is chosen here for illustration as this has previously been shown to possess the highest crosstalk of the ten amplified signals following C-FOPA amplification [3]. This is because the high frequency region of the amplified signal spectrum generates FWM crosstalk not only from signal-signal interactions, but also from second order interactions between the original signals and newly generated signal-pump-signal waves surrounding the pump [19]. In addition, the particular dispersion and hence phase-matching conditions of the HNLF influence the crosstalk distribution. For the pump/signal frequency combination described in this work, the crosstalk within the signal band is maximum at 194.4THz, although this may not be a general rule for WDM amplification in C-FOPAs using different sets of signal bands and/or pump frequencies and/or HNLF properties. The pump powers were optimised as follows: 0.2km-C-FOPA – 33.4 dBm PP; 0.2km-RA-FOPA – 28.5 dBm PP & 37 dBm RP; 1km-C-FOPA – 29.5 dBm PP; 1km-RA-FOPA – 24.5 dBm PP & 32 dBm RP. It can be seen that there is an inflection point in the S-to-X ratio profile. This occurs where the crosstalk power begins to dominate the ASE floor. Note that in the case of the C-FOPA, this point always occurs after a shorter distance than the equivalent RA-FOPA. This results in a 7 dB and 10 dB difference of the S-to-X ratio between C-FOPA and RA-FOPA for the 0.2 km and 1 km lengths of HNLF respectively. The absolute crosstalk power is also seen to be significantly lower (higher S-to-X ratio) in the 0.2 km length RA-FOPA over the 1 km RA-FOPA by approximately 10 dB.

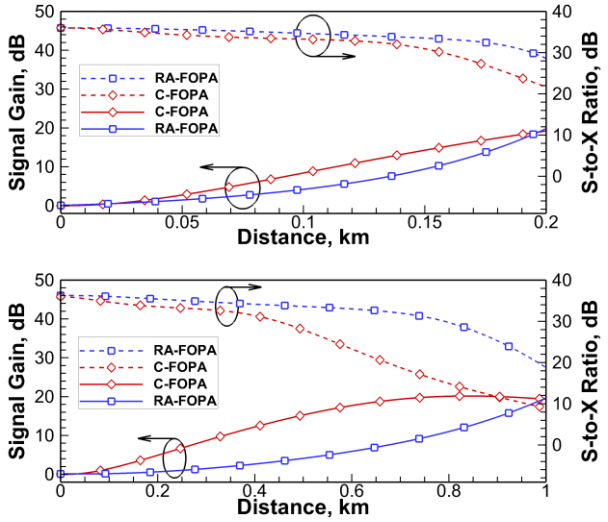

Fig. 4. Signal gain and S-to-X ratio along the HNLF for a C-FOPA and RA-FOPA with different length of HNLF. Per-signal input power is -10 dBm and average net-gain is 20 dB.

Figure 5 shows the evolution dynamics of the S-to-X ratio at 194.4 THz along the HNLF for 20 dB net-gain and different Raman/parametric pump power ratios. It can be seen that the crosstalk level decreases with increased Raman pump power for both 0.2 km- and 1 km-RA-FOPA due to the lower required power of the parametric pump. This results in a 7 dB and 15 dB difference of the S-to-X ratio between C-FOPA and RA-FOPA when using the maximum Raman pump power simulated for the 0.2 km and 1 km lengths of HNLF respectively. It should also again be noted that significant suppression of absolute FWM crosstalk power is obtained by reducing the highly nonlinear fibre interaction length for the same net-gain if no other parameters are changed.

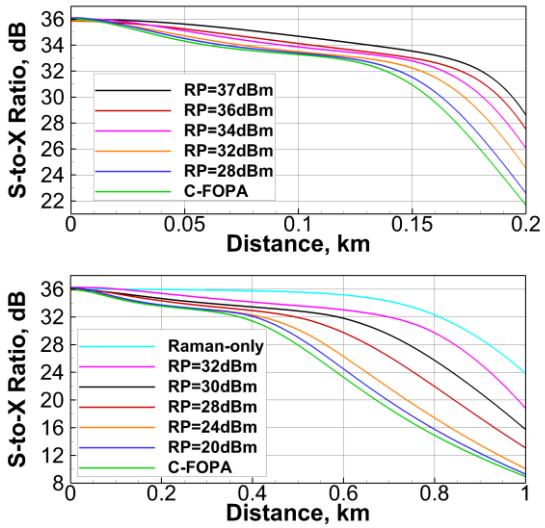

Fig. 5. S-to-X ratio along the HNLF for a C-FOPA and different configuration of RA-FOPA with different length of HNLF. Per-signal input power is -10 dBm and average net-gain is 20 dB.

5. Crosstalk vs gain level in RA-FOPA

To examine how the crosstalk evolution depends on the RA-FOPA gain, simulations of the 0.2km-RA-FOPA were performed for different net-gain conditions as follows: a) 15 dB gain with 24.8 dBm PP & 37 dBm RP b) 20 dB gain with 28.5 dBm PP & 37 dBm RP and c) 25 dB gain with 30.6 dBm PP & 37 dBm RP.

Figure 6 shows the resulting signal gain and S-to-X ratio profiles for 194.4 THz along the HNLF. It can be seen that as might be expected from standard theory the crosstalk level increases with signal gain due to FWM products power being proportional to the interacting power of the signals. In all cases, for minimised crosstalk the RP power has been maximised to an experimentally-achievable 37 dBm and any extra gain required being provided by adjusting the level of PP power. It can be seen that employing even shorter HNLF lengths may offer scope for further reduced crosstalk, but the reduced interaction length would require compensation with greater PP power. The overall result is therefore not easily predictable without further simulations and is moreover likely to be experimentally challenging due to SBS considerations and high-power tolerant filter availability.

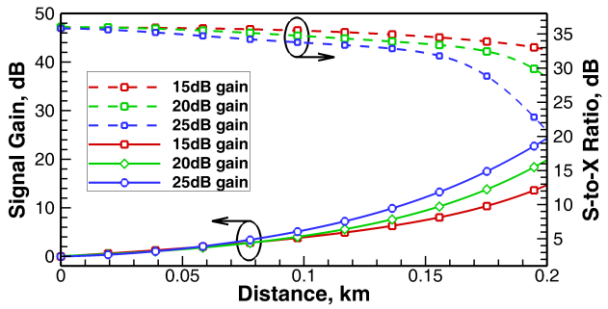

Fig. 6. Signal gain and S-to-X ratio along the HNLF for RA-FOPA with different average net-gain.

Figure 7 shows how S-to-X-ratio depends on signal gain level for 193.5 THz and 194.4 THz WDM-signals. Solid symbols correspond to the C-FOPA (15 dB gain – 32.4 dBm PP, 20 dB gain – 33.4 dBm PP, 25 dB gain – 34.4 dBm PP) whilst open symbols correspond to the RA-FOPA with the Raman/parametric pump power ratios adjusted as follows (in order of reduced spread or higher Raman contribution): a) 15 dB gain – 28/31.8, 29/31.6, 30/31.4, 31/31.1, 32/30.7, 33/30.2, 34/29.6, 35/28.6, 36/27.2, 37/24.8 dBm b) 20 dB gain – 26/33.1, 28/32.9, 30/32.6, 32/32.1, 34/31.2, 36/29.7, 37/28.5 dBm c) 25 dB gain – 26/34.1, 28/33.9, 30/33.7, 32/33.2, 34/32.6, 36/31.5, 37/30.6 dBm. It can be seen that the level of FWM product at the high frequency side of the spectrum is consistently higher than at the low frequency side. This is a result of an unequal satisfaction of the phase-matching conditions between different WDM-signals involved in the FWM processes, combined with the impact of pump-signal interactions and second-order mixing. In the C-FOPA case, this results in a 5 dB, 9 dB and 14 dB spread of the S-to-X ratio between the 193.5 THz and 194.4 THz WDM-signals for the 15 dB, 20 dB and 25 dB signal gains respectively. For the RA-FOPA simulated with the stated pump power levels, the crosstalk spread can be seen to be reduced at each gain level as the contribution from the Raman pump is increased, resulting in complete suppression/equalisation in the 15dB case. For the higher gains, the reduction in spread is lessened, even at maximum Raman contribution. At 20dB gain, the spread is reduced to ~3dB (from 9dB C-FOPA), and at 25dB it is reduced to ~7.5dB (from 14dB C-FOPA).

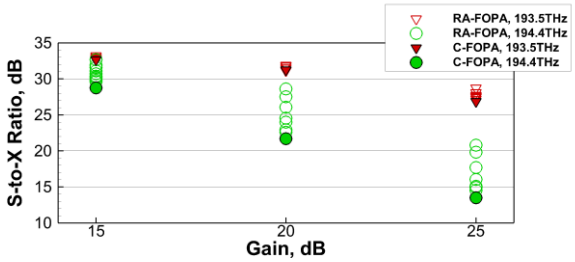

Fig. 7. S-to-X ratio for a C-FOPA and RA-FOPA and different average net-gain. Per-signal input power is -10 dBm and HNLF length is 0.2 km.

6. Crosstalk vs signal channel count in RA-FOPA

Finally, the impact of the number of signals and their grid spacing on the crosstalk growth was investigated. Fig. 8 shows S-to-X ratio dynamics for the signal at 194.4 THz in both 10x100 GHz and 20x50 GHz WDM scenarios through a 0.2 km HNLF and with 20 dB net-gain. The per-signal input power was the same in the 10 and 20 channel cases, i.e. the total input power was doubled in the 20 channel case. Pump powers were: a) C-FOPA with 33.4 dBm PP b) RA-FOPA1 with 31.2 dBm PP & 34 dBm RP and c) RA-FOPA2 with 28.5 dBm PP & 37 dBm RP. It can be seen that independent of amplifier type, the crosstalk level starts to grow much sooner (in distance) for the 20x50 GHz signals over the 10x100 GHz signals. As is known [20], FWM crosstalk power scales as N^2, where N – number of channels in the WDM signal. This results in ~6 dB discrepancy in crosstalk levels between 10x100 GHz and 20x50 GHz signals at the output. It is clear that the RA-FOPAs provide reduced crosstalk over the C-FOPA for both channel counts.

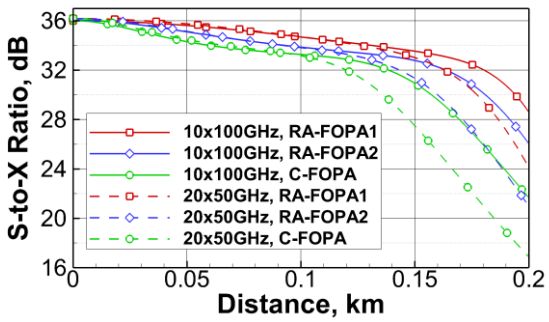

Fig. 8. S-to-X ratio along the HNLF for 20 dB average net-gain of 10x100GHz and 20x50GHz WDM-signals.

7. Conclusion

We have characterised WDM QPSK signal amplification and FWM crosstalk generation for the first time in both conventional C-FOPAs and RA-FOPAs, achieving close agreement between simulation and experimental data. The RA-FOPA showed reduced crosstalk over the C-FOPA for fixed gain, HNLF length and channel count conditions. A maximum reduction of 10 dB was seen within the explored parameter-space, and is likely to be more significant at higher channel counts. Furthermore, the crosstalk dependence on HNLF length has been explored in the RA-FOPA. A significant 10 dB reduction in crosstalk was seen when reducing the HNLF length from 1 km to 0.2 km for 20 dB net-gain amplification of 10x58 Gb/s, 100 GHz-spaced signals. Similar RA-FOPA improvements were seen over the C-FOPA for three different net-gain conditions (15, 20 and 25 dB) and for two different channel grid spacings (100 and 50 GHz). In terms of optimum pump power ratio for the RA-FOPA, the lowest crosstalk was spectrally achieved using the highest Raman power available – in practise it is expected however for high gains that issues of double Rayleigh scattering would cause signal corruption before these FWM crosstalk-optimum Raman powers are reached. This has not been the focus of the research presented here and will be addressed in a future paper. In summary therefore, potential has been demonstrated for the RA-FOPA to be a viable future WDM optical amplifier in new regions of the transmission spectrum.

Acknowledgments

This work was partially funded by the UK EPSRC grant EP/J009709/2 and the Ministry of Education and Science of the Russian Federation (no. RFMEFI57814X0029).